Journal of Biomolecular NMR (2005) 32: 129–139
DOI 10.1007/s10858-005-5093-6

Article

Resolution enhanced homonuclear carbon decoupled triple resonance experiments for unambiguous RNA structural characterization

Kwaku T. Dayie[a,b,c,*]
[a]*Department of Molecular Genetics and Program in Structural Biology, Lerner Research Institute, Cleveland Clinic Foundation, Cleveland, OH, 44195, USA;* [b]*Cleveland Center for Structural Biology, Cleveland, OH, 44195, USA;* [c]*Department of Biochemistry, Case Western Reserve University, Cleveland, OH, 44195, USA*

Received 3 January 2005; Accepted 21 March 2005

Key words: adiabatic pulses, band-selective homonuclear decoupling, heteronuclear cross-polarization, RNA NMR assignment strategy, scalar coupling

Abstract

Large RNAs (>30 nucleotides) suffer from extensive resonance overlap that can seriously hamper unambiguous structural characterization. Here we present a set of 3D multinuclear NMR experiments with improved and optimized resolution and sensitivity for aiding with the assignment of RNA molecules. In all these experiments strong base and ribose carbon–carbon couplings are eliminated by homonuclear band-selective decoupling, leading to improved signal to noise and resolution of the C5, C6, and C1′ carbon resonances. This decoupling scheme is applied to base-type selective ^{13}C-edited NOESY, ^{13}C-edited TOCSY (HCCH, CCH), HCCNH, and ribose H1C1C2 experiments. The 3D implementation of the HCCNH experiment with both carbon and nitrogen evolution enables direct correlation of ^{13}C and ^{15}N resonances at different proton resonant frequencies. The advantages of the new experiments are demonstrated on a 36 nucleotides hairpin RNA from domain 5 (D5) of the group II intron *Pylaiella littoralis* using an abbreviated assignment strategy. These four experiments provided additional separation for regions of the RNA that have overlapped chemical shift resonances, and enabled the assignment of critical D5 bulge nucleotides that could not be assigned using current experimental schemes.

Introduction

An arsenal of multi-nuclear NMR experiments exists for assigning resonances in RNA molecules (Dieckmann and Feigon, 1994; Pardi, 1995; Varani et al., 1996; Wijmenga and van Buuren, 1998; Cromsigt et al., 2001; Lukavsky and Puglisi, 2001; Furtig et al., 2003). Of these, experiments that connect exchangeable and nonexchangeable protons (Simorre et al., 1995; Fiala et al., 1996; Simorre et al., 1996; Sklenar et al., 1996; Wöhnert et al., 2003) or relay information within the ribose ring (Heus et al., 1994; Dayie et al., 1998; Wijmenga and van Buuren, 1998; O'Neil-Cabello et al., 2004a) are particularly versatile. When combined with ^{15}N/^{13}C-edited NOESY and TOCSY, these through-bond experiments provide unambiguous complete assignment for exchangeable protons and partial assignment for non-exchangeable protons in small (<24 nucleotides) RNA molecules. Invariably all these experiments include one or two carbon evolution periods. This ^{13}C-evolution is advantageous in RNA of little resonance overlap. Nevertheless, use of ^{13}C isotopic enrichment introduces one-bond carbon–carbon splitting of the C5 and C6 signals in pyrimidine bases and for all the carbons in the ribose ring. These splittings in turn complicate spectral analysis, especially for large RNAs. As a remedy, constant time frequency editing experiments are

*To whom correspondence should be addressed. E-mail: dayiek@ccf.org

used to eliminate these carbon–carbon line splittings (Bax et al., 1979; Bax and Freeman, 1981; Grzesiek and Bax, 1992; van de Ven and Philippens, 1992). Their use, however, limits the acquisition time that can be employed ($t_1^{max} \leq (J_{C5C6} = 67\ Hz)^{-1}$, $(J_{C1'C2'} = 43\ Hz)^{-1}$), and the resulting long constant-time delay needed for adequate resolution usually leads to significant loss of signal for large RNA molecules.

Here, we present four three-dimensional experiments with increased resolution and sensitivity for a fully $^{13}C/^{15}N$ labeled RNA. Instead of the constant-time editing, we incorporate the alternative decoupling scheme of adiabatic band-selective ^{13}C–^{13}C decoupling (Kupce and Wagner, 1996; Brutscher et al., 2001). In a new 3D version of the (H)C-TOCSY-(C)NH experiment (Simorre et al., 1995; Sklenar et al., 1996; Wöhnert et al. 2003), the C5 (or C6) carbons are selectively decoupled from the C6 (or C5) carbons. Similarly in highly resolved C1′-selected NOESY, CCH-TOCSY (Heus et al., 1994; Dayie et al., 1998), and H1C1C2 (O'Neil-Cabello et al., 2004a) experiments the C1′ carbons are decoupled from the C2′ carbons. These four experiments enabled the resolution of most of the ambiguities in assigning a 36 nucleotides hairpin RNA from domain 5 of the group II intron *Pylaiella littoralis* (Costa et al., 1997), hereafter referred to as D5 RNA, that has extensive overlap of the base C6 and ribose C1′ carbon and N6 amino nitrogen resonances.

Materials and methods

Sample preparation

Fully $^{13}C/^{15}N$ labeled and U base-specific labeled RNA samples were synthesized by *in vitro* transcription with T7 RNA polymerase from synthetic DNA templates (Operon Technologies, Inc, Alameda, CA) and with isotopically labeled NTPs (Isotec, OH) using established protocols (Milligan et al., 1987; Milligan and Uhlenbeck, 1989; Batey et al., 1995; Puglisi and Wyatt, 1995). An N-terminal His-tag containing T7 RNA polymerase was overexpressesed in *Escherichia coli* BL21 (DE3) and purified on a Ni-chelating sepharose column (Pharmacia). The DNA promoter sequence, or top strand, has a C nucleotide at the –18 T7 promoter region (Baklanov et al., 1996) (CTOP) and has the sequence: 5′ CTA ATA CGA CTC ACT ATA G. The corresponding template strand, or bottom strand, used for NMR analysis was 5′-g AAC CGT ACG TGC GAC TTT CAT CGC ATA CGG CTC c TAT AGT GAG TCG TAT TAG-3′ (lower case letters represent non-native nucleotides introduced to improve transcription yield and they do not affect the catalytic ability of this domain (data not shown)). Use of methyl nucleotides at the 3′-end substantially reduced the amount of $N + 1$ and higher add-on transcripts (Kao et al., 1999). The optimal transcription conditions, found by a systematic sparse matrix variation of Mg^{2+}, NTP, and enzyme concentrations, were 15 mM total NTP and 13.7 mM Mg^{2+} in a transcription buffer of 40 mM Tris–HCl, pH 8.1, 1 mM spermidine, 5 mM dithiothreitol (DTT), 0.01% Triton X-100, 80 mg/ml PEG 8000, 300 nM each DNA strand, and 1.5 µl T7 polymerase (optimized amount) per 40 µl of transcription volume. After 3 h of incubation at 310 K, the transcription reaction was extracted with phenol/chloroform/isoamyl alcohol (25:24:1) to remove the T7 RNA polymerase, followed by ethanol precipitation. The crude RNA precipitate was purified using denaturing preparative gel electrophoresis. The product band was detected by briefly UV shadowing the gel, excised, and electro-eluted in an Elutrap electro-separation system (Schleicher and Schuell). The purified RNA was precipitated with sodium acetate/ ethanol, washed and dried. The lyophilized RNA stocks were resuspended in water and dialyzed in a Biodialyzer (Nestgroup, Cambridge, MA) with a 500 MWCO membrane (Nestgroup, Cambridge, MA) for 12–24 h each against 0.5 M potassium chloride, 10 mM EDTA, and then 0.1 mM EDTA, and finally against two changes of ddH_2O water. After dialysis, the RNA was lyophilized, and resuspended into NMR buffer (100 mM KCl, 10 mM potassium phosphate pH 6.2, 8% D_2O (or 100%), with or without 3 mM $MgCl_2$, trace of sodium azide). For accurate determination of the RNA concentration, a small sample was hydrolyzed in 1.0 M sodium hydroxide, neutralized with HCl, and the UV absorbance was used to calculate the concentration. NMR sample volumes were 250 µl in shigemi tubes, and ranged in concentration from 0.3 mM to 1.8 mM.

NMR experiments

NMR experiments were run on four channel $^{UNITY}INOVA$ 500 and 600 MHz spectrometers equipped with actively shielded *z*-axis gradient triple resonance probes, and NMR data sets were processed using the NMRpipe program (Delaglio et al., 1995) and the peak positions and intensities were analyzed with Sparky program (Goddard and Kneller, 2004). NMR experiments were recorded at temperatures from 278 to 308 K. Resonance assignments were obtained with heteronuclear multidimensional NMR experiments such as 2D (^{1}H, ^{15}N) HSQC and TROSY, 2D (^{1}H, ^{13}C) HSQC and TROSY, 2D (^{1}H, ^{15}N) CT-HSQC and CT-TROSY, 2D (^{1}H, ^{13}C) CT-HSQC and CT-TROSY (Pervushin et al., 1997; Brutscher et al., 1998; Meisnner and Sorensen, 1999; Rance et al., 1999), 2D/3D bi-directional HCN (Hu et al., 2001), 2D HCNCH, 2D HCCNH, 2D HCCNH-TOCSY (Simorre et al., 1995, 1996; Fiala et al., 1996; Sklenar et al., 1996), 3D AH2, H8 HCCH-COSY TROSY (Simon et al., 2001), 3D (^{1}H,^{13}C, ^{1}H) HCCH-COSY and HCCH-TOCSY (Clore et al., 1990; Fesik et al., 1990; Kay et al., 1990; Heus et al., 1994; Matsuo et al., 1996; Dayie et al., 1998), 3D (^{1}H,^{1}H, ^{15}N) NOESY-HSQC, 3D (^{1}H,^{1}H, ^{13}C) NOESY-HSQC, 3D (^{1}H,^{1}H, ^{13}C) NOESY-HSQC (Clore et al., 1990; Pascal et al., 1994), and H1C1C2 experiment (O'Neil-Cabello et al., 2004a). To optimize resolution, the 3D (H)C-TOCSY-(C)NH, HCCH-TOCSY, NOESY-HSQC, and H1C1C2 experiments were modified to incorporate homonuclear carbon-carbon decoupling as described below.

Results and discussion

We present four modified triple resonance experiments with improved and optimized resolution and sensitivity for aiding with the assignment of RNA molecules. In all these experiments, eliminating the carbon–carbon coupling by homonuclear band-selective decoupling improved the signal to noise and resolution of the C6 and C1′ carbon regions of the D5 RNA. The proposed experiments, in concert with other experiments, allowed us to unambiguously assign all the pyrimidine resonances that appear in the ^{15}N- and ^{13}C-HSQC spectra for a 1 mM D5 RNA at 25 °C as detailed below.

3D ^{13}C and ^{15}N edited (H)C-TOCSY-(C) NH RNA experiment

The pulse sequence employed for carbon-decoupled 3D ^{13}C and ^{15}N edited (H)C-TOCSY-(C)NH (or cd-HCCNH), shown in Figure 1a, differs in some important details from previous implementations. Previous 2D versions evolve either the proton or carbon resonances separately, and in a pseudo 3D cytidine optimized experiment both amino protons and C6 carbon resonances are frequency labeled during the t_1 evolution period and C6 carbons are decoupled from the C5 carbons with selective pulses (Simorre et al., 1995; Sklenar et al., 1996). This 3D cd-HCCNH evolves both carbon and nitrogen resonances in the t_1 and t_2 periods. Similar to the 2D version, the 3D cd-HCCNH starts with magnetization on aromatic protons and then transfers these via INEPT to the attached carbons. The resulting antiphase carbon magnetization (C5 or C6) is refocused into inphase magnetization and labeled with its chemical shift during the carbon evolution period. Unlike earlier versions, homonuclear band-selective decoupling is applied to either C4 and C5 or C6 to eliminate the carbon-carbon coupling ($^1J_{C5C6}\sim$ 67 Hz) and thereby achieve high resolution in the aromatic C5/C6 carbon regions. Because the spectral regions of C4, C5 and C6 are well separated (C4-C5: ~68 ppm, C5-C6: ~40 ppm) with small bandwidths (~6 ppm), we used the constant adiabacity WURST-2 pulse that has high selectivity and minimum RF power requirements (Kupce and Wagner, 1996). The inphase carbon magnetizations (C5 or C6) are then transferred to C4 by a homonuclear TOCSY of either 6.5 or 13 ms depending on whether the C5 or C6 magnetization is desired. Rather than simultaneously transferring from C5 and C6, we prefer transferring from either C5 (~100 ppm) or C6 (~141 ppm). This latter arrangement enabled us to maximize the resolution enhancement afforded by the narrower (~3 ppm) spectral width for each region instead of larger (~42 ppm) spectral region required for the former. The drawback, compared to an earlier version that provided simultaneous correlations of H6C6/H5C5 in one experiment (Wöhnert et al., 2003), is that here two

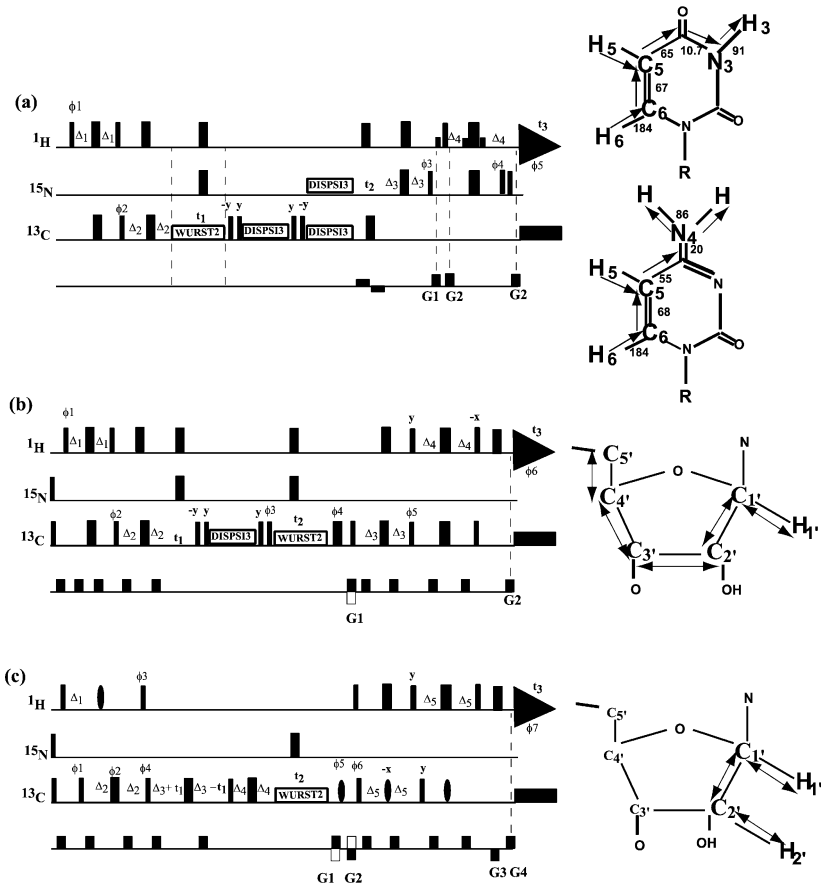

experiments have to be recorded. Nonetheless, in cases of extensive overlap, it is preferable and advantageous to record either a C5 or C6 selective experiment (Supplementary Figure 1). The C4 magnetization is then transferred to N3 (uridine) or N4 (cytosine) by a 50 ms C, N DIPSI-3 cross-polarization sequence (Bertrand et al., 1978; Muller and Ernst, 1979). The resulting inphase N3/N4 magnetization is frequency labeled and transferred to inphase imino/amino protons. A WATERGATE water suppression scheme (Piotto et al., 1992) is used to eliminate the water resonance. In the current 3D implementation, C5/C6 carbon and N3/N4 nitrogen are correlated with H3/H4 proton resonances. Overcoming the strong carbon–carbon coupling (~67 Hz) with homonuclear band-selective decoupling improved the signal to noise and resolution of the C6 carbon region of D5 RNA. For example, the proposed 3D experiment is quite sensitive requiring ~28 h for uridine and cytidine optimized experiments involving $^{15}N/^{13}C/^{1}H$ evolution periods for a ~1 mM D5 RNA sample. These acquisition times are comparable to those obtained using earlier 2D versions correlating either H5 and H6 or C5 and C6 with the imino or amino protons (Supplementary Figure 1) (Wöhnert et al., 2003).

Ambiguities in assignment still remained using the earlier HCCNH experiments for our 36 nucleotide RNA (Figure 2a). The imino proton of U9 located in the bulge region of D5, for instance, was unobservable using previous experiments (Figure 2b) under comparable acquisition conditions. Using our proposed 3D cd-HCCNH experiment, the U9 imino proton could be correlated with its aromatic carbon and imino nitrogen resonances from the 2D projection spectra of the 3D experiment (Figure 2c,d). Similarly for the overlapped amino and aromatic resonances (Figure 3b), the new 3D experiments proved critical. The resolution afforded by ^{15}N–^{13}C planes at different ^{1}H frequencies for the severely

Figure 1. 3D experiments with band-selective homonuclear decoupling. All rectangular ^{1}H pulses were applied with 35.5 kHz field, while ^{13}C and ^{15}N were applied with 15.2 and 4.6 kHz, respectively. Narrow and wide bars represent nonselective 90 and 180° pulses, respectively. All pulses are applied with an x phase, unless indicated. (a) 3D (H6/H5) C6/C5(C4)NH pulse sequence for recording 3D ^{13}C and ^{15}N-edited spectra on fully ^{15}N,^{13}C labeled RNA. On the 500 MHz, the ^{13}C to ^{15}N magnetization transfer is accomplished by a 45.4 ms DISPSI-3 sequence at an RF field strength of 1.9 kHz, and homonuclear carbon–carbon transfer using a DISPSI-3 TOSCY sequence at an RF field strength of 10 kHz of 5.8, 14.4, and 19 ms duration depending on whether C5 or C6 or both C5 and C6 transfers were desired. The ^{15}N frequency was set to 160 ppm (98 ppm) for imino (amino) nitrogen resonances for the duration of the sequence. The ^{13}C frequency was set to 175 ppm for the ^{15}N–^{13}C hetero-TOCSY transfer and to 135 ppm for the ^{13}C homonuclear TOCSY transfer, and C5 (U: 98 ppm or C: 104 ppm) or C6 (at 141 ppm) chemical shift evolution period. For adiabatic decoupling a WURST pulse length of 3 ms (< 1/5 JCC) was used, and the waveforms were calculated to cover bandwidths of 12 ppm. The C5 region was decoupled with a 1500 bandwidth centered at 100 ppm and the C6 region was decoupled with a 1500 bandwidth centered at 141 ppm. An additional waveform was applied at 165 ppm for the low field aromatic carbon resonances. Delay parameters used are: 1.5 s recycle delay, transfer delays of $\Delta_1 = 1/4J_{CH} = 1.38$ ms, $\Delta_2 = \Delta_1 = \Delta_3 = \Delta_4 = 1/4J_{NH} = 2.6$ ms for Uridines and $\Delta_3 = \Delta_4 = 1/8J_{NH} = 1.3$ ms for cytidines. GARP was used for ^{15}N decoupling with RF field strength of 2 kHz. The phase cycle used is $\phi1 = x, -x$, $\phi2 = 2x, -2x$, $\phi3 = 4x, -4x$, $\phi4 = 8x, -8x$, and $\phi5$ = receiver = *ab*, $a = x, -2x, x$; $b = -a$. Quadrature detection in $^{13}C(t_1)$ and $^{15}N(t_2)$ is achieved by States-TPPI of $\phi2$, and $\phi3$ respectively. For ^{1}H–^{1}H evolution, quadrature detection in $^{1}H(t_1)$ is achieved by States-TPPI of $\phi1$, with decoupling pulses applied on the carbon and nitrogen channels. Shown on the right hand side of the pulse program is a schematic representation of the magnetization transfer within cytidine and uridine aromatic rings. The numbers indicate the coupling constants (Hz) between nuclei involved in the coherence transfer (Ippel et al., 1996). (b) Pulse sequence for C1′-selective and C2′-decoupled sensitivity-enhanced CCH TOCSY experiment. A DISPSI-3 sequence at an RF field strength of 7 kHz for the homonuclear TOSCY transfer using 18–25 ms depending on whether C1′ to C4′ or C1′ to C5′ transfers are desired. The ^{1}H and ^{15}N carriers are centered at water and 200 ppm, respectively. The ^{13}C frequency was set to 80 ppm for the first carbon evolution period and the ^{13}C homonuclear TOCSY transfer; thereafter it is shifted to 92.5 ppm for the second carbon chemical shift evolution period. For adiabatic decoupling a WURST pulse length of 3 ms (< 1/5 JCC) was used, and the waveforms were calculated to cover bandwidths of 8 ppm for the C2′ region using a B_1 (rms) field strength of 253 Hz at 500 MHz ^{1}H frequency. Delay parameters used are: 1.5 s recycle delay, transfer delays of $\Delta_1 = \Delta_2 = \Delta_3 = \Delta_4 = 1/4J_{CH=1.38}$ ms. GARP was used for ^{13}C decoupling with RF field strength of 4.5 kHz. The phase cycle used is $\phi1 = y, -y$, $\phi2 = 2x, -2x$, $\phi3 = 4x, -4x$, $\phi4 = 8x, -8x$, $\phi5 = y$, and $\phi6$ = receiver = *ab*, $a = x, -2x, x$; $b = -a$. Quadrature detection in $^{13}C(t_1)$ achieved by States-TPPI of $\phi2$; for $^{13}C(t_2)$ this is accomplished in a Rance-Kay fashion: two fids are acquired for each t_2 increment with the amplitude of G_1 and the phase $\phi5$ inverted for the second FID. The strengths and durations of the coherence selection gradients are G_1 = (13 G/cm, 2.0 ms), and G_2 = (12.93 G/cm, 500 μs). Shown on the right hand side of the pulse program is a schematic representation of the magnetization transfer within the ribose ring. A coupling of ~42 Hz mediates the coherence transfer among the carbon atoms and ~160 Hz for the protonated carbons (Ippel et al., 1996). (c) Pulse sequence for C1′-selective and C2′-decoupled H1C1C2 experiment. The ^{1}H and ^{15}N carriers are centered at water and 200 ppm, respectively. The ^{13}C frequency was set to 75 ppm for the first carbon evolution period and thereafter it is shifted to 92.5 ppm for the second carbon chemical shift evolution period. Shaped pulses are of the 180° rSNOB variety (Kupce et al., 1996) and have durations of 1.54 ms (centered on H1′ with a B_1 rms field strength of 673.6 Hz) and 1.36 ms (on C1′ with a B_1 rms field strength of 762.8 Hz) at 600 MHz ^{1}H frequency. Delay parameters used are: 1.5 s recycle delay, transfer delays of $\Delta_1 = 1/2J_{C1'H1'}$, $\Delta_2 = 1/4J_{C1'C2'}$, $\Delta_3 = 1/2J_{C1'C2'}$, $\Delta_4 = 1/4J_{C1'C2'}$, and $\Delta_5 = 1/4J_{C1'H1'}$. GARP was used for ^{13}C decoupling with RF field strength of 4.5 kHz. All rectangular ^{1}H pulses were applied with 31.4 kHz field, while ^{13}C and ^{15}N were applied with 10.2 kHz and 6.4 kHz respectively. The phase cycle used is $\phi1 = y$, $\phi2 = -4y, 4x$, $\phi3 = 2y, -2y$, $\phi4 = x$, $\phi5 = 4y, -4y, 4x, -4x$, $\phi6 = -x$, and $\phi7$ = receiver = *abba*, $a = x, -2x, x$; $b = -a$. Quadrature detection in $^{13}C(t_1)$ achieved by States-TPPI increment of $\phi1$, $\phi2$, $\phi4$; for $^{13}C(t_2)$ this is accomplished in a Rance-Kay fashion: two fids are acquired for each t_2 increment with the amplitude of G_1 and G_2 and the phase $\phi6$ inverted for the second FID. The strengths and durations of the coherence selection gradients are $G_1 = G_2$ = (13 G/cm, 1.0 ms), and $G_3 = G_4$ = (12.93 G/cm, 250 μs). Shown in the right hand side of the pulse sequence is a schematic representation of the magnetization transfer between the ribose carbon C1′ and C2′ atoms and their directly attached protons. A coupling of ~42 Hz mediates the coherence transfer among the carbon atoms and ~160 Hz for the protonated carbons (Ippel et al., 1996).

overlapped resonances is depicted in Figure 3. The overlapped C4, C5, C11, and C27 resonances (Figure 3b) are properly resolved. It may appear paradoxical that we can resolve aromatic carbon resonances within 0.1– 0.2 ppm of each other (Figure 3). Consider that the aromatic C6 carbon sweep width used in the cytidine-optimized experiment is only 2.5 ppm. By acquiring 16 complex points and extending this to 32 points by linear prediction, we obtain a digital resolution of 0.04 ppm/point in the carbon dimension. Consequently we do not observe any bleed-through from the other resonances within each plane depicted in Figure 3a. As described below, identifying these missing resonances enabled further assignment in a ^{13}C C2′-selectively decoupled and edited NOESY.

3D base-type selective high-resolution ^{13}C-edited NOESY HSQC experiment

To make maximum use of the resolved resonances from the C6 region afforded by the previous experiment, we run base-type selective ^{13}C-edited NOESY HSQC with a carbon–carbon filter just

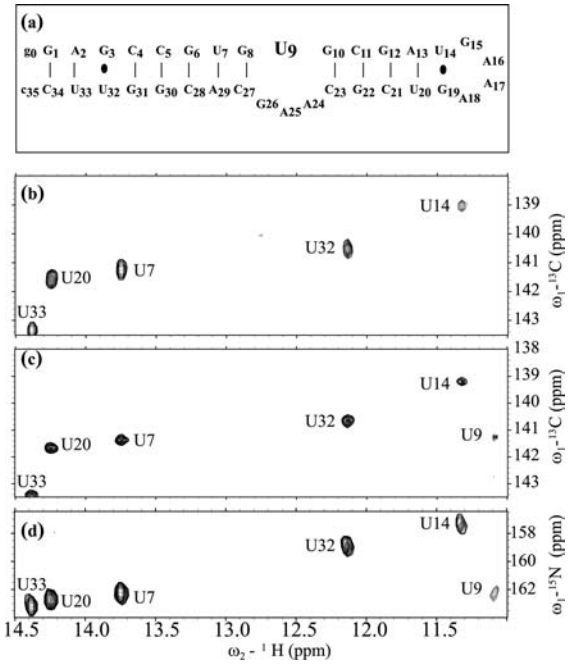

Figure 2. (a). Secondary structural scheme for the 36mer D5 RNA enzyme derived from the group II intron RNA of *Pyllaeilla littoralis* used in these studies. Hydrogen-bonded base pairs for which imino protons are observed and or direct hydrogen-bonded contacts are observed from an HNN-COSY experiment are indicated with solid lines. (b) 2D spectrum correlating Uridine imino aromatic C6 carbon resonances using the sequence of Wöhnert et al., 2003 modified to run with constant-time editing. The 2D experiment was acquired with 82*1024 complex points in t_1 and t_2, respectively. A relaxation delay of 1 s, a constant time delay of 14 ms, 512 scans per t_1 increment, and spectral widths of 6400 Hz in F1 and 13000 Hz in F2 were used. Note the absence of the U9 resonance. (c) 2D projection spectrum of the 3D cd-HCCNH experiment depicting imino proton and aromatic C6 correlations. The 3D spectrum was acquired with 4*16*512 complex points in t_1, t_2 and t_3, respectively. A relaxation delay of 1 s, 256 scans per increment, and spectral widths of 405 Hz in F1, 754 Hz in F2, and 13000 Hz in F3 were used. Note the elusive U9 resonance is clearly visible. (d) 2D projection spectrum of the 3D cd-HCCNH experiment depicting imino proton and nitrogen correlations. Acquisition parameters are listed in (c). Note the highly overlapped U9 resonance is clearly resolved.

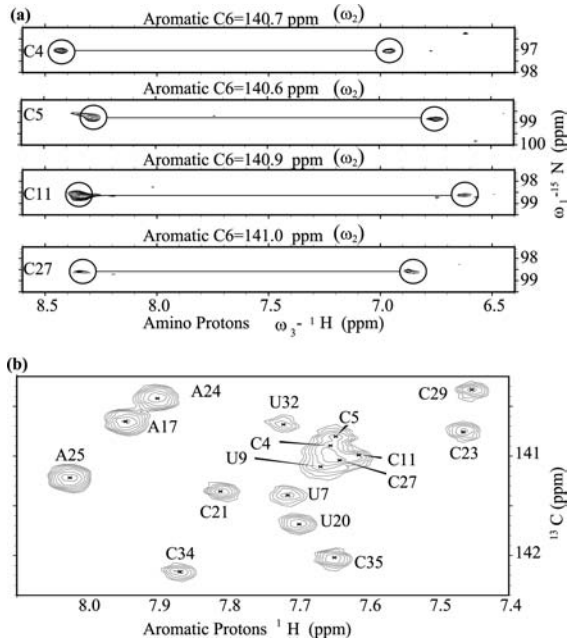

Figure 3. (a) 2D strip plots (ω_1 = ^{15}N, ω_3 = ^{1}H) of the 3D cd-HCCNH experiment recorded on the 36 nucleotide D5 RNA with the pulse sequence of Fig. 1a. Carbon planes corresponding to the severely overlapped resonances of C4, C5, C11, and C27 (See Fig. 3b) are clearly resolved. The 3D spectrum was acquired with 16*16*512 complex points in t_1, t_2 and t_3, respectively. A relaxation delay of 1 s, 128 scans per increment, and spectral widths of 304 Hz in F1, 679 Hz in F2, and 13000 Hz in F3 were used. (b) ^{1}H–^{13}C HSQC correlation spectrum of D5 RNA recorded with homonuclear multiple band selective decoupling. Only part of the aromatic H6-C6 and H8-C8 region is shown. Note the unusual degree of overlap of the four nucleotides C4, C5, C11, and C27. The 2D experiment was acquired with 128*512 complex points in t_1 and t_2, respectively. A relaxation delay of 1 s, 16 scans per t_1 increment, and spectral widths of 1257 Hz in F1 and 6600 Hz in F2 were used.

after the first INEPT step and prior to the carbon evolution period. This experiment helped to separate C6 pyrimidine resonances from C8 purine resonances and uridine from cytidine base resonances. Such a set-up has been described previously for ^{13}C-edited TROSY NOESY (Brutscher et al., 2001). During the carbon evolution period a multi-band-selective homonuclear decoupling was implemented as described above. For the base-selective experiments, two separate experiments were recorded with and without the decoupling of the C5 band during the carbon–carbon filter using WURST-2 waveforms. Limiting the selective decoupling band to the uridine C5 band enables the separation of the uridine from the cytidine base resonances. Identical results are obtained using either a uridine-specific labeled sample or the carbon–carbon filtering (Figure 4). Accordingly, this NMR technique complements the more time consuming and costly biochemical method of specific and selective labeling.Use of the carbon filtering proved critical for disentangling six cytosine resonances that overlapped with three uridine resonances in D5 RNA and provided an independent confirmation of the assignment of the

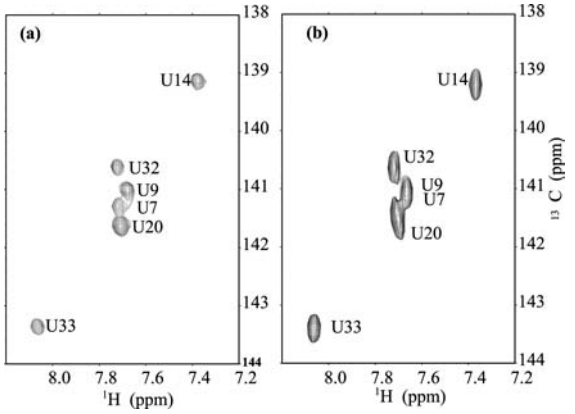

Figure 4. (a) Aromatic ^{1}H–^{13}C HSQC correlation spectra for D5 RNA on fully labeled D5 using homonuclear multiple band selective decoupling together with a uridine carbon-carbon filter as described in the text. The 2D experiment was acquired with 128*512 complex points in t_1 and t_2, respectively. A relaxation delay of 1 s, 16 scans per t_1 increment, and spectral widths of 3318 Hz in F1 and 6600 Hz in F2 were used. (b) Aromatic ^{1}H–^{13}C constant-time TROSY correlation spectra for D5 RNA on uridine-specific labeled D5. Identical spectra are obtained in both cases. The 2D experiment was acquired with 88*512 complex points in t_1 and t_2, respectively. A relaxation delay of 1 s, a constant time delay of 14 ms, 32 scans per t_1 increment, and spectral widths of 6940 Hz in F1 and 5498 Hz in F2 were used. Note that the TROSY spectrum was referenced identically to the HSQC spectrum for ease of comparison.

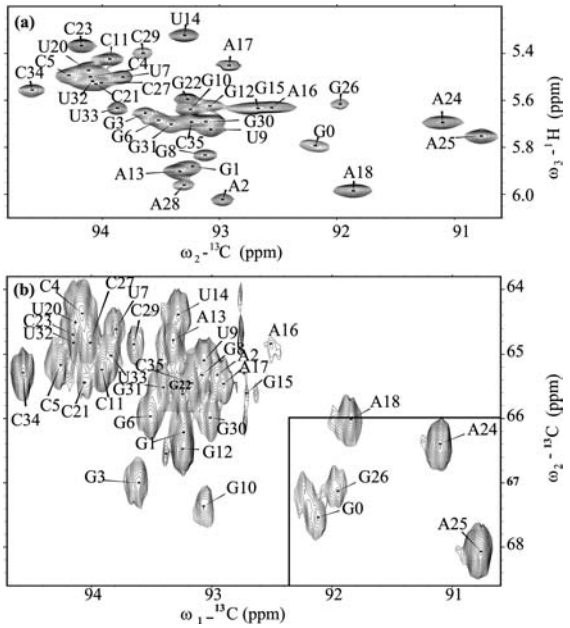

Figure 5. 2D projection spectra of 3D experiments depicting correlation maps of (a) C1′-H1′ in the C1′-selected ^{13}C-edited NOESY HSQC and (b) C5′-C1′ in the c2pd-CCH TOCSY. Note the very high resolution obtained in the C1′ region using the multi-band selective decoupling. G19 resonates at a proton frequency of 3.8 ppm outside the spectral region depicted, and is therefore not shown. The 3D NOESY spectrum was acquired with 45*64*256 complex points in t_1, t_2 and t_3, respectively, on an Inova 600 MHz spectrometer. A relaxation delay of 1 s, 16 scans per increment, and spectral widths of 800 Hz in F1, 3200 Hz in F2, and 5000 Hz in F3 were used. The 3D TOCSY spectrum was acquired with 81*64*256 complex points in t_1, t_2 and t_3, respectively, on Inova 500 MHz spectrometer. A relaxation delay of 1 s, 8 scans per increment, and spectral widths of 754.3 Hz in F1, 4903.2 Hz in F2, and 5000 Hz in F3 were used.

severely overlapped U9 resonance assigned with the cd-HCCNH experiment (Figure 3b).

In addition to the overlap in the base region, the ribose C1′-region can also be very crowded for large RNAs. This poses a challenge for the NOESY-based RNA sequential assignment strategy (Feigon et al., 1983; Scheek et al., 1983; Nikonowicz and Pardi, 1993). To circumvent this overlap problem, we not only used WURST-2 decoupling of C2′ resonances during the carbon evolution period, as described previously for ^{13}C-edited TROSY NOESY (Brutscher et al., 2001), but also incorporated a C1′-selective 180° rSNOB pulse into the ^{13}C-edited NOESY. That arrangement allowed us to sample a much reduced sweep width of 5.5 ppm instead of 10 ppm with a concomitant improvement in resolution in a highly overlapped H1′/C1′ region of D5 RNA (Figure 5a). In principle, one could fold the spectrum along the carbon dimension without the need for selective pulses. However, to achieve comparable reduced spectral width of ~5 ppm necessitates folding C5 resonances of U and C back into the C1′ region. In favorable cases there would be no overlap with C1′ peaks; in the case of D5 RNA, these peaks overlap. Use of C1′ selective pulses then becomes an attractive alternative for such cases. With a highly resolved H1′/C1′ filter for the NOESY, unambiguous mapping of all the ribose H1′-to-base connectivities for all 36 nucleotides within D5 RNA was achieved. The 2D C1′-H1′ projection of this 3D experiment (Figure 5a) is then very useful to interpret other experiments such as HCCH TOCSY described below.

3D high-resolution ^{13}C-edited HCCH TOCSY experiment

Using the improved C1′-selected and C2′-decoupled NOESY, we were able to correlate all the

sequential H1′ to H2/H6/H8 NOEs. However to extend the assignment to the rest of the resonances within the ribose ring (H2′–H5′/H5″), it is necessary to unambiguously assign the remaining ribose resonances. We modified a previously proposed CCH TOCSY experiment (Dayie et al., 1998). Instead of constant time editing for the two carbon evolutions periods, we imposed a non-constant time for the first carbon evolution period before the CC-TOCSY mixing period, and thereafter we applied a C2′-selective decoupling waveform for the second carbon evolution period (Figure 1b). The C2′ signals were decoupled using WURST-2 sequence, as described above, and the ribose C1′ selective pulse was effected with an rSNOB shape (Kupce et al., 1996). We call this C2′ decoupled sequence c2pd-CCH TOCSY. Selecting the C1′ signal during the second carbon evolution period allowed us to sample a much reduced sweep width (89–95 ppm) with increased resolution compared to a constant-time or non-decoupled version. From the C1′ plane we could easily read off all the other carbon frequencies from C2′, C3′, C4′ and C5′ in a ladder form (Heus et al., 1994; Dayie et al., 1998). The 2D projection of C5′ onto C1′ resonance region lifts some of the C5′ chemical shift overlap found in a traditional H5′/H5″-C5′ spectral region (Figure 5b). This experimental arrangement enabled the assignment of all the ribose carbons at the well-resolved H1′/C1′ resonances. Armed with this unambiguous carbon information, it is then relatively simple to interpret any of the standard HCCH-COSY, HCCH-RELAY COSY, and HCCH TOCSY to extract the proton chemical shifts of the directly attached carbons. Another attractive alternative is to use a C1′-selective HCCH TOCSY experiment, similar to the Cbd-HCCH-TOCSY proposed for protein applications (Matsuo et al., 1996). In our hands this provided an easier assignment for all the resonances than combining both COSY and RELAY-COSY (data not shown).

This information then helps with re-interpreting the NOESY data beyond the H1′ proton region and other subsequent experiments such as residual dipolar and or scalar couplings. For example, the ribose carbon chemical shifts contain very valuable sugar puckering information that is apparent from C1′–C5′ carbon spectrum (Figure 5b) (Ebrahimi et al., 2001). The plot shown in Figure 5b visually highlights nucleotides with potential C2′-endo (S-type) puckering, and it predicts S-type pucker for the bulge nucleotides A24, A25, and G26. Thus unambiguous assignment of these ribose resonances will go a long way in improving the structural characterization of RNA molecules.

3D high-resolution optimized H1C1C2 experiment

Once all the protonated ribose and base atoms are assigned unambiguously, that information can to be used for other downstream applications such as relaxation or coupling measurements. A recently proposed "out-and-back" experiment allows the measurement of five scalar and dipolar couplings and features two constant evolution periods (O'Neil-Cabello et al., 2004a). This valuable experiment has limited resolution for RNAs larger than a 24mer because of constant time editing during both C1′ and C2′ evolution periods. To improve the resolution in the C1′ dimension, we replaced the second constant time evolution period with a refocusing period that transfers C2′ magnetization to C1′. The second carbon evolution period now proceeds with C2′ decoupling using WURST-2 sequence and a ribose C1′ selective pulse effected with a rSNOB shape (Kupce et al., 1996), as described above (Figure 1c). We call this sequence c2pd-H1C1C2. Selecting the C1′ signal during the second carbon evolution period allowed us to sample, once again, a much reduced sweep width (89–95 ppm) with increased resolution compared to the constant-time version (Figure 6). The rSNOB C1′ selective pulse is used to preserve the bandwidth and reduce potential artifacts introduced by homonuclear decoupling (Kupce et al., 1996). The overlapped resonances, G6 and G30 for instance, are better resolved in the C2pd-H1C1C2 spectra. A drawback of this implementation, however, is reduction in sensitivity because of the separation of the evolution period from the refocusing period. Nonetheless, all cross peaks visible in the regular spectrum are present in the c2pd-H1C1C2 spectrum. As discussed previously, the sign of $^{2}J_{C1'H2'}$ is critical for distinguishing S-type (negative $^{2}J_{C1'H2'}$) from N-type (positive $^{2}J_{C1'H'}$) sugar pucker (Ippel et al., 1996), and the isotropic values of $^{1}J_{C1'H1'}$, $^{2}J_{C1'H2'}$ and $^{3}J_{H1'H2'}$ likely correlate with ribose ring pucker (Ippel et al., 1996; Podlasek et al., 1996; O'Neil-Cabello et al., 2004a). Detailed assessment of the values of all three couplings and the deduced

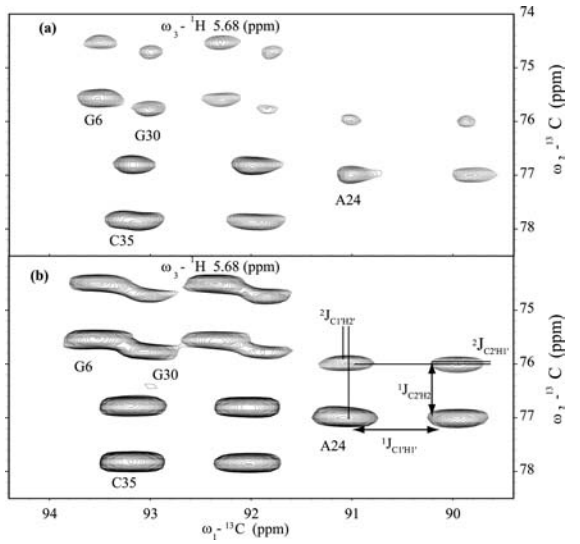

Figure 6. Cross-sections taken through a 600 MHz 3D H1C1C2 NMR spectrum of D5 RNA shown in Fig. 2a recorded with (a) a C1′-selected and C2′-decoupled t_2 (C1′) evolution c2pd-H1C1C2 version and (b) constant-time evolution period of 11.7 ms ($\Delta_3 = 1/4J_{C1'C2'}$ for optimal signal-to-noise) for C1′ using the original sequence. Both experiments were acquired with 30*32*512 complex points in t_1, t_2 and t_3, respectively. A relaxation delay of 1 s, 16 scans per increment, spectral widths of 1358 Hz in F1, 1509 Hz in F2, and 6600 Hz in F3 were used in (a), and spectral widths of 3123 Hz in F1, 1509 Hz in F2, and 6600 Hz in F3 were used in (b). Separation between multiplet components corresponding to $^1J_{C1'H1'}$, $^1J_{C2'H2'}$, $^2J_{C1'H2'}$ and $^2J_{C2'H1'}$ are marked. Peaks in the c2pd-H1C1C2 spectrum are better resolved but weaker than those in the regular spectrum.

ribose pucker values derived from the original experiment, from cross-correlated measurements (Boisbouvier et al., 2000), and from chemical shift analysis will be presented elsewhere (Dayie, K.T., Eldho, N.V, and Seetharaman, M, personal communication). Contrary to previous X-ray and NMR study reports on a very closely related D5 RNA hairpin from yeast (Zhang and Doudna, 2002; Sigel et al., 2004), our current results suggest all three bulge nucleotides A24, A25, and G26 adopt a C2′-endo conformation.

An approach for unambiguous assignment using resolution optimized experiments

With these modified experiments described above, an abbreviated assignment strategy can be proposed, compared to previous schemes (Feigon et al., 1983; Scheek et al., 1983; Nikonowicz and Pardi, 1993; Dieckmann and Feigon, 1997; Cromsigt et al., 2001). We have successfully applied this strategy to assign the medium sized D5 RNA (36 nt) as follows.

(1) Establish secondary structure

(a) Perform imino-imino walk in helical region using ^{1}H–^{1}H NOESY aided by ^{15}N HSQC (2D ^{1}H–^{1}H and 3D ^{15}N-edited NOESYs).

(b) Use the direct dual hydrogen bond experiments (Dingley and Grzesiek, 1998; Luy and Marino, 2000) to validate base-pair formation. Regular helical segments were rapidly identified.

(c) Identify Cytidine's H4 amino, Guanosine's H3 and Uracil's H1 imino protons, and Adenine's H2 contacts from the homouclear ^{1}H–^{1}H NOESY and 2D ^{13}C, ^{15}N HSQC to use for subsequent through-bond assignment.

(2) Link exchangeable with non-exchangeable resonances

(a) Use the imino and amino proton information from (1) to identify Uracil's and Cytidine's H6, H5 resonances in 2D ^{1}H–^{1}H HCCNH experiment (Simorre et al., 1995; Sklenar et al., 1996; Wöhnert et al., 2003).

(b) Resolve ambiguities with resolution optimized 3D cd-HCCNH experiments described in this work.

(c) Link aromatic proton and carbon resonances using resolution optimized 3D cd-HCCNH experiments described in this work.

(d) Identify Guanosine's imino protons with base H8 resonances with 2D HCCNH experiment (Fiala et al., 1996; Simorre et al., 1996; Sklenar et al., 1996).

(3) Link adenine H2 and H8 resonances

(a) Use HSQC and HCCH RELAY COSY TROSY (Simon et al., 2001).

(4) Link base protons with ribose H1′/C1′ resonances

(a) Armed with all the base proton information from (1) to (3), link these base protons with ribose C1′/H1′ resonances

with the bi-directional HCN experiment (Hu et al., 2001). If necessary, use N1 and N9 aromatic nitrogen as a filter to reduce chemical shift overlap.

(b) Perform sequential base-ribose NOESY walk using C1′-selected C2-decoupled and resolution optimized 3D−^{13}C edited NOESY (Brutscher et al., 2001) described in this work.

(5) Extend C1′/H1′ assignment to rest of resonances within the ribose ring

(a) Using H1′/C1′ assignments derived from the analysis from (4), extend the assignment to the rest of the ribose ring using HCCH TOCSY.

(b) Resolve ambiguities with resolution optimized c2pd-CCH TOCSY experiment presented in this work and Cbd-HCCH TOCSY (Matsuo et al., 1996) adapted for nucleic acids.

(6) Iteratively resolve remaining assignment ambiguities

(a) Using assignments from (1) to (5), reinterpret C1′-selected and resolution optimized 3D−^{13}C edited NOESY (Brutscher et al., 2001; this work) for sequential walk.

(b) Use carbon–carbon filtered experiments and or nucleotide specific labels in resolution optimized 3D−^{13}C edited NOESY (Brutscher et al., 2001).

(c) Use ^{1}H−^{1}H NOESY at multiple temperatures aided by C1′- and C8-/C6- selected and resolution optimized ^{13}C HSQC at equivalent temperatures.

(7) Supplement with phosphorus assignments

(a) Use HCP for non-structured regions (Heus et al., 1994; Marino et al., 1994; O'Neil-Cabello et al., 2004b).

Conclusions

By incorporating homonuclear band-selective decoupling into a number of multinuclear NMR experiments, the resulting resolution and sensitivity enhancement can prove critical for aiding the assignment and structural characterization of RNA molecules. In particular, the 3D implementation of the cd-HCCNH experiment with both carbon and nitrogen evolution enables direct correlation of ^{13}C and ^{15}N resonances at different proton resonant frequencies. For our 36 nucleotide RNA, this experimental set-up enabled the assignment of critical bulge nucleotides that could not be assigned unambiguously using current experimental schemes. Additionally using this band-selective decoupling strategy in a few key RNA experiments (^{13}C edited NOESY, ^{13}C-edited TOCSY, H1C1C2), an RNA assignment strategy outlined above can be implemented to help with structural characterization of RNA molecules, as well as automation of RNA structural analysis process.

Supporting information available

Figures showing 2D spectra of previous HCCNH experiment correlating (a) uridine imino and H5/H6 resonances; (b) uridine imino and aromatic C5/C6 carbon resonances run with constant-time editing; (c, d) cytidine amino and C5 (c) and C6 (d) resonances. This material is available at http://dx.doi.org/10.1007/s10858-005-5093-6.

Acknowledgements

I thank Dr. Eldho Nadukkudy for preparing the doubly labeled RNA samples, Die Wang, Drs. Hua Li, Marian Peris, Orlando Gumbs, and Mahadevan Seetharaman for preparing the T7 RNA polymerase, Dr. Rick Padgett for the generous gift of a His-tagged T7 RNA polymerase construct, and Dr. Eriks Kupce for many discussions on selective pulse shaping. I am grateful to Drs. Frank Sönnichsen and Jun Qin for critical comments and reading of the manuscript. The work is supported by NSF grant (MCB-0316783) and start-up funds from Cleveland Clinic Foundation to K.T.D.

References

Baklanov, M.M., Golikova, L.N. and Malygin, E.G. (1996) *Nucl. Acid Res.*, **24**, 3659–3660.

Batey, R.T., Battiste, J.L. and Williamson, J.R. (1995) *Methods Enzymol.*, **261**, 300–322.

Bax, A., Mehlkopf, A.F. and Smidt, J. (1979) *J. Magn. Reson.*, **35**, 167–169.
Bax, A. and Freeman, R. (1981) *J. Magn. Reson.*, **44**, 542–561.
Bearden, D.W. and Brown, L.R. (1989) *Chem. Phys. Lett.*, **163**, 432–436.
Bertrand, R.D., Moniz, W.B., Garroway, A.N. and Chingas, G.C. (1978) *J. Am. Chem. Soc.*, **100**, 5227–5229.
Boisbouvier, J., Brutscher, B., Pardi, A., Marion, D. and Simorre, J.-P. (2000) *J. Am. Chem. Soc.*, **122**, 6779–6780.
Braunschweiler, L. and Ernst, R.R. (1983) *J. Magn. Reson.*, **53**, 521–528.
Brutscher, B., Boisbouvier, J., Pardi, A., Marion, D. and Simorre, J.P (1998) *J. Am. Chem. Soc.*, **120**, 11845–11851.
Brutscher, B., Boisbouvier, J., Kupce, E., Tisne, C., Dardel, F., Marion, D. and Simorre, J.P. (2001) *J. Biomol. NMR*, **19**, 141–151.
Costa, M., Fontaine, J.M., Loiseaux-de Goer, S. and Michel, F. (1997) *J. Mol. Biol.*, **274**, 353–364.
Clore, G.M., Bax, A., Driscoll, P.C., Wingfield, P.T. and Gronenborn, A.M. (1990) *Biochemistry*, **29**, 8172–8184.
Cromsigt, J., van Buuren, B., Schleucher, J. and Wijmenga, S. (2001) *Methods Enzymol.*, **338**, 371–399.
Dayie, K.T., Tolbert, T.J. and Williamson, J.R. (1998) *J. Magn. Reson.*, **130**, 97–101.
Delaglio, F., Grzesiek, S., Vuister, G.W., Zhu, G., Pfeifer, J. and Bax, A. (1995) *J. Biomol. NMR*, **6**, 277–293.
Dieckmann, T. and Feigon, J. (1994) *Curr. Opin. Struct. Biol.*, **4**, 745–749.
Dieckmann, T. and Feigon, J. (1997) *J. Biomol. NMR*, **9**, 259–272.
Dingley, A.J. and Grzesiek, S. (1998) *J. Am. Chem. Soc.*, **120**, 8293–8297.
Ebrahimi, M., Rossi, P., Rogers, C. and Harbison, G.S. (2001) *J. Magn. Reson.*, **150**, 1–9.
Feigon, J., Leupin, W., Denny, W.A. and Kerns, D.R. (1983) *Biochemistry*, **22**, 5943–5951.
Fesik, S.W., Eaton, H.L., Olejniczak, E.T., Zuiderweg, E.R.P., McIntosh, L.P. and Dahlquist, F.W. (1990) *J. Am. Chem. Soc.*, **112**, 886–888.
Fiala, R., Jiang, F. and Patel, D.J. (1996) *J. Am. Chem. Soc.*, **118**, 689–690.
Furtig, B., Richter, C., Wöhnert, J. and Schwalbe, H. (2003) *Chembiochem.*, **4**, 936–962.
Goddard, T.D. and Kneller, D.G. (2004) *SPARKY 3*, University of California, San Francisco.
Grzesiek, S. and Bax, A. (1992) *J. Magn. Reson.*, **96**, 432–440.
Heus, H.A., Wijmenga, S.S., Van De Ven, F.J. and Hilbers, C.W. (1994) *J. Am. Chem. Soc.*, **116**, 4983–4984.
Hu, W., Gosser, Y.Q., Xu, W. and Patel, D.J. (2001) *J. Biomol. NMR*, **20**, 167–172.
Ippel, J.H., Wijmenga, S.S., de Jong, R., Heus, H.A., Hibers, C.W., de Vroom, E., van der Marel, G.A. and van Boom, J.H. (1996) *Magn. Reson. Chem.*, **34**, S156–S176.
Kao, C., Zheng, M. and Rudisser, S. (1999) *RNA*, **5**, 1268–1272.
Kay, L.E., Ikura, M. and Bax, A. (1990) *J. Am. Chem. Soc.*, **112**, 888–889.
Kupce, E. and Wagner, G. (1996) *J. Magn. Reson. B.*, **110**, 309–312.
Lukavsky, P.J. and Puglisi, J.D. (2001) *Methods*, **25**, 316–332.
Luy, B. and Marino, J.P. (2000) *J. Am. Chem. Soc.*, **122**, 8095–8096.
Marino, J.P., Schwalbe, H., Anklin, C., Bermel, W., Crothers, D.M. and Griesinger, C. (1994) *J. Am. Chem. Soc.*, **116**, 6472–6473.
Matsuo, H., Kupce, E. and Wagner, G. (1996) *J. Magn. Reson. B*, **113**, 190–194.
Meissner, A. and Sorensen, O.W. (1999) *J. Magn. Reson.*, **139**, 439–442.
Milligan, J.F., Groebe, D.R., Witherell, G.W. and Uhlenbeck, O.C. (1987) *Nucl. Acid Res.*, **15**, 8783–8798.
Milligan, J.F. and Uhlenbeck, O.C. (1989) *Methods Enzymol.*, **180**, 51–62.
Mueller, L. and Ernst, R.R. (1979) *Mol. Phys.*, **38**, 963–992.
Nikonowicz, E.P. and Pardi, A. (1993) *J. Mol. Biol.*, **232**, 1141–1156.
O'Neil-Cabello, E., Bryce, D.L., Nikonowicz, E.P. and Bax, A. (2004a) *J. Am. Chem. Soc.*, **126**, 66–67.
O'Neil-Cabello, E., Wu, Z., Bryce, D.L., Nikonowicz, E.P. and Bax, A. (2004) *J. Biomol. NMR*, **30**, 61–70.
Pardi, A. (1995) *Methods Enzymol.*, **261**, 350–380.
Pascal, S.M., Muhandiram, D.R., Yamazaki, T., Forman-Kay, J.D. and Kay, L.E. (1994) *J. Magn. Reson. B*, **103**, 197–201.
Pervushin, K., Riek, R., Wider, G. and Wuthrich, K. (1997) *Proc. Natl. Acad. Sci. USA.*, **94**, 12366–12371.
Piotto, M., Saudek, V. and Sklenar, V. (1992) *J. Biomol. NMR*, **2**, 661–665.
Podlasek, C.A., Wayne, A.S., Carmichael, I., Shang, M., Basu, B. and Serianni, A.S. (1996) *J. Am. Chem. Soc.*, **118**, 1413–1425.
Puglisi, J.D. and Wyatt, J.R. (1995) *Methods Enzymol.*, **261**, 323–350.
Rance, M., Loria, J.P. and Palmer, A.G. 3rd (1999) *J. Magn. Reson.*, **136**, 92–101.
Scheek, R.M., Russo, N., Boelens, R. and Kaptein, R. (1983) *J. Am Chem. Soc.*, **105**, 2914–2916.
Sigel, R.K., Sashital, D.G., Abramovitz, D.L., Palmer, A.G. III, Butcher, S.E. and Pyle, A.M. (2004) *Nat. Struct. Mol. Biol.*, **11**, 87–192.
Simon, B., Zanier, K. and Sattler, M. (2001) *J. Biomol. NMR*, **20**, 173–176.
Simorre, J.P., Zimmermann, G.R., Pardi, A., Farmer, B.T. 2nd and Mueller, L. (1995) *J. Biomol. NMR*, **6**, 427–432.
van de Ven, F.J.M. and Philippens, M.E.P. (1992) *J. Magn. Reson.*, **97**, 637–644.
Varani, G., Aboul-ela, F. and Allain, F.H.T. (1996) *Prog. NMR Spectrosc.*, **29**, 51–127.
Wijmenga, S.S. and van Buuren, B.N.M. (1998) *Prog. NMR Spectrosc.*, **32**, 287–387.
Wöhnert, J., Gorlach, M. and Schwalbe, H. (2003) *J. Biomol. NMR.*, **26**, 79–83.
Zhang, L. and Doudna, J.A. (2002) *Science*, **295**, 2084–2088.